

# The discretization of a current and a magnetic field by a superconducting structure with an asymmetric quantum interferometer

Cite as: Fiz. Nizk. Temp. **45**, 1068–1077 (August 2019); doi: [10.1063/1.5116543](https://doi.org/10.1063/1.5116543)  
Submitted: 25 June 2019



View Online



Export Citation



CrossMark

S. I. Bondarenko,<sup>a)</sup> V. N. Fenchenko, V. P. Koverya, and A. V. Krevsun

## AFFILIATIONS

B. Verkin Institute for Low Temperature Physics and Engineering, National Academy of Sciences of Ukraine, 47 Nauka Ave., Kharkov 61103, Ukraine

<sup>a)</sup>Email: [bondarenko@ilt.kharkov.ua](mailto:bondarenko@ilt.kharkov.ua)

## ABSTRACT

A mathematical model of the quantum processes in an asymmetric interferometer with an ultralow inductance  $L_0 \approx 10^{-13}$  H, shunted by a highly inductive superconducting circuit  $L_1 \gg L_0 \times 10^7$  is constructed. The model is verified by comparing the calculated parameters of the model with the experimentally measured values.

Published under license by AIP Publishing. <https://doi.org/10.1063/1.5116543>

## 1. INTRODUCTION

Devices based on superconducting quantum interferometers, known as SQUIDS, are widely used for highly sensitive magnetic measurements,<sup>1–4</sup> and in recent years more and more attention has been paid to using SQUIDS as elements of computing technology.<sup>5</sup> One important direction in such application is the creation of superconducting devices that provide the conversion of analog electrical quantities into their discrete values. This type of discrete transformation of current and magnetic field analog values can be implemented by a structure proposed by us in Refs. 6–8, which is an asymmetric dc superconducting quantum interferometer, shunted by a superconducting circuit with a high inductance.

After the discovery of the Josephson effect,<sup>9</sup> the current distribution in superconducting circuits with Josephson contacts, their current and magnetic states were studied mainly via dc quantum interferometers, with branch inductances being limited by the ratio  $E_M \gg E_T$  between the magnetic energy of the quantization circuit  $E_M \approx \Phi_0^2 / (2L_0)$  ( $L_0$  is the interferometer inductance,  $\Phi_0$  is the magnetic flux quantum) and the energy of the thermal perturbation processes  $E_T \approx kT$  ( $k$  is the Boltzmann constant,  $T$  is the temperature). In order for the interferometer to work at  $T = 4.2$  K, it is necessary that its inductance  $L_0$  be less than  $10^{-9}$  H. If the inductance of the interferometer is greater, then it loses its properties due to thermal fluctuations. This is why there has been a lack of interest in studying the critical current states and reaction

to the external magnetic field of superconducting circuits, with Josephson contacts having much higher inductance values than that of an interferometer.

However, such circuits contain quantum phenomena that were previously unknown, which explains the recently increased interest in the study of their current characteristics. In particular, asymmetric dc superconducting quantum interferometers (with two Josephson point contacts of different critical currents) shunted by a superconducting circuit with significant inductance, make it possible to perform simultaneous measurements of key superconductor parameters, such as the width of their bandgap and the relaxation time of the superconducting state. As is known, the width of the bandgap determines the maximum possible speed of Cooper pair displacement, and thus the critical current density of the superconductor, whereas the relaxation time of the superconducting state limits the maximum speed of superconductor-based devices. These types of measurements are based on two basic concepts, which are the theoretical predictions of A. Silver and J. Zimmerman.<sup>10–12</sup> The first prediction is that the voltage pulse on a superconducting quantum interferometer during the discrete switching of its circulating current is proportional to the bandgap of the superconductor. The second is proposed in Ref. 8, and concerns extending the voltage pulse duration to a value that can be easily measured by shunting the interferometer with a highly inductive superconducting circuit (significantly greater than  $10^{-9}$  H).

Note that studies on the current states in quantum interferometers shunted by inductors<sup>13</sup> have been performed before. However, only inductors from non-superconducting metals have been considered. A mathematical description of the processes taking place in a quantum interferometer shunted by a superconducting inductor is not yet available, which limits the ability to simultaneously measure the bandgap of the superconductor and the relaxation time of the superconducting state.

The purpose of this article is to build a theory for the processes occurring in an asymmetric dc superconducting quantum interferometer with an extremely low inductance  $L_0 \approx 10^{-13}$  H, shunted by a highly inductive superconducting circuit  $L_1 \gg L_0 \times 10^7$ , during the passage of a direct current or the application of magnetic field.

## 2. THE MATHEMATICAL MODEL OF A SHUNTED ASYMMETRIC INTERFEROMETER

The main characteristics of an asymmetric interferometer (Fig. 1) shunted by a highly inductive superconducting circuit are: the dependence of the current flowing through the shunt circuit on the magnitude of the transport current, the flux of the external magnetic field through the shunt circuit, and the magnitude and duration of the voltage pulses generated on the shunt circuit.

Because the inductance of the interferometer is much less than the inductance of the shunt circuit, before reaching the critical value, the current  $I_i$  flowing through the interferometer represents the sum of the transport current  $I_0$  and the current in the shunt circuit  $I_1$ , caused by the external magnetic field  $H$

$$I_i = I_0 + I_1. \quad (1)$$

On the other hand, the current  $I_i$  is the sum of the currents flowing through the parallel-connected Josephson contacts. Therefore, due to the stationary Josephson effect in the case of a contact's current sinusoidal dependence on the phase difference

$$I_i = I_a \sin \varphi_a + I_b \sin \varphi_b, \quad (2)$$

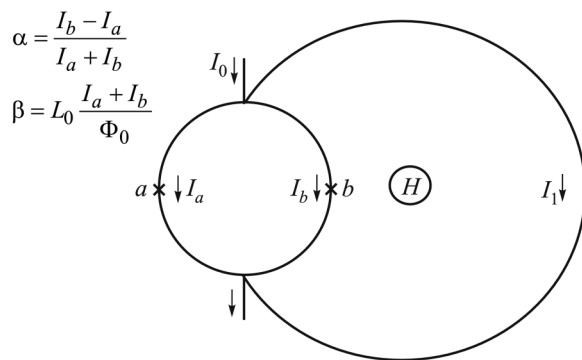


FIG. 1. An asymmetric interferometer shunted by a superconducting inductor.

where,  $\varphi_a, \varphi_b$  are the phase differences of the order parameter at the contacts, and  $I_a, I_b$  are the critical currents of the contacts.

Equation (1) must be supplemented by the condition that the wave function be unique when traversing the interferometer circuit

$$\frac{\varphi_a - \varphi_b}{2\pi} = -\frac{\Phi}{\Phi_0}, \quad (3)$$

where  $\Phi = \Phi_e + L_0 I_s$  is the total magnetic flux through the interferometer circuit,  $\Phi_e$  is the external magnetic flux,  $L_0$  is the interferometer inductance, and  $I_s$  is the circulating screening current in the interferometer. It is related to the Josephson currents flowing through the contacts via the expression<sup>14</sup>

$$I_s = \frac{L_a I_a \sin \varphi_a - L_b I_b \sin \varphi_b}{L_0}, \quad (4)$$

where the coefficients  $L_a, L_b$  correspond to the inductances of the interferometer arms. Thus, the condition of wave function uniqueness when it traverses the interferometer circuit, assuming the inductance in the interferometer's left and right arm is equal, and that there is zero external magnetic flux  $\Phi_e$ , looks like

$$\frac{\varphi_a - \varphi_b}{\pi} + L_0 \frac{I_a \sin \varphi_a - I_b \sin \varphi_b}{\Phi_0} = 0. \quad (5)$$

It should be noted here that the external magnetic flux  $\Phi_e$  required to analyze the currents flowing through interferometers, including those that are asymmetric, in the studies conducted by other authors.<sup>14,15</sup> In our case, this flux is zero. The magnitude of the interferometer's critical current, the distribution of currents in the interferometer, and its magnetic flux, are determined only by the total transport current through the interferometer, and the degree of asymmetry of its contacts' critical currents. This required the development of a new method for analyzing the current states of an asymmetric interferometer, which is described below.

Let us normalize the currents to the sum of the contacts' critical currents, determine the interferometer asymmetry parameter  $\alpha = (I_b - I_a)/(I_b + I_a)$ ,  $|\alpha| < 1$ , and introduce the parameter  $\beta = L_0(I_b + I_a)/\Phi_0$ . Then the currents  $i_a, i_b$  that flow through the interferometer arms are defined by the following expressions:

$$\begin{cases} i_a = \frac{1 - \alpha}{2} \sin \varphi_a, \\ i_b = \frac{1 + \alpha}{2} \sin \varphi_b, \end{cases} \quad (6)$$

the total current through the interferometer is

$$i = \frac{(1 - \alpha) \sin \varphi_a + (1 + \alpha) \sin \varphi_b}{2}, \quad (7)$$

the circulating current is

$$i_s = \frac{(1 - \alpha) \sin \varphi_a - (1 + \alpha) \sin \varphi_b}{4}, \quad (8)$$

the magnetic flux

$$f_s = \beta \frac{(1 - \alpha) \sin \varphi_a - (1 + \alpha) \sin \varphi_b}{4}, \quad (9)$$

and the wave function uniqueness condition when traversing the interferometer circuit is

$$\varphi_a - \varphi_b + \frac{\pi\beta}{2} [(1 - \alpha) \sin \varphi_a - (1 + \alpha) \sin \varphi_b] = 0. \quad (10)$$

Determining the critical current of the interferometer is reduced to finding the maximum of the transport current together with the wave function uniqueness condition when traversing the interferometer circuit. This problem can be solved using the method of indefinite Lagrange multipliers, which consists of reducing this task to the problem of finding the unconditional extremum of an auxiliary function.<sup>16</sup> This function is a linear combination of the expression for the transport current  $f$  and the condition  $\varphi_i$  for the uniqueness of the wave function, taken by  $\lambda_i$  with a coefficient  $\lambda$  known as the Lagrange multiplier,

$$F = \frac{(1 - \alpha) \sin \varphi_a + (1 + \alpha) \sin \varphi_b}{2} + \lambda \left\{ \varphi_a - \varphi_b + \frac{\pi\beta}{2} [(1 - \alpha) \sin \varphi_a - (1 + \alpha) \sin \varphi_b] \right\}, \quad (11)$$

and let us make a system of equations, setting equal to zero the partial derivatives of the obtained function with respect to,  $\varphi_a$ ,  $\varphi_b$ ,  $\alpha$  and  $\lambda$

$$\begin{cases} \frac{\partial F}{\partial \varphi_a} = \frac{(1 - \alpha) \cos \varphi_a}{2} + \lambda \left\{ 1 + \frac{\pi\beta}{2} (1 - \alpha) \cos \varphi_a \right\} = 0, \\ \frac{\partial F}{\partial \varphi_b} = \frac{(1 + \alpha) \cos \varphi_b}{2} - \lambda \left\{ 1 + \frac{\pi\beta}{2} (1 + \alpha) \cos \varphi_b \right\} = 0, \\ \frac{\partial F}{\partial \lambda} = \varphi_a - \varphi_b + \frac{\pi\beta}{2} [(1 - \alpha) \sin \varphi_a - (1 + \alpha) \sin \varphi_b] = 0. \end{cases} \quad (12)$$

Eliminating  $\lambda$ , we transform the system to the form

$$\begin{cases} \frac{\cos \varphi_a}{1 + \alpha} + \frac{\cos \varphi_b}{1 - \alpha} + \pi\beta \cos \varphi_a \cos \varphi_b = 0, \\ \varphi_a - \varphi_b + \frac{\pi\beta}{2} [(1 - \alpha) \sin \varphi_a - (1 + \alpha) \sin \varphi_b] = 0. \end{cases} \quad (13)$$

The values of the order parameter phase difference, which we denote  $\varphi_a^*$ ,  $\varphi_b^*$ , correspond to the extremum of function (11) when condition (10) is fulfilled, and are among the solutions to system (13). In particular, a sufficient condition for this is the negativity of the second differential of the Lagrange function.

For a symmetric interferometer in the absence of an external field, the critical current is equal to the sum of the Josephson contact critical currents, and this current obviously does not create any magnetic flux.

For an asymmetric interferometer, the critical current is

$$i_c = i_a \sin \varphi_a^* + i_b \sin \varphi_b^* \quad (14)$$

and generally speaking, it is less than the sum of the critical contact currents, and the magnetic flux created by the critical current is non-zero

$$f_s = \beta \frac{i_a \sin \varphi_a^* - i_b \sin \varphi_b^*}{2}. \quad (15)$$

Note that if the difference in the critical currents of the Josephson contacts is small ( $|\alpha\beta| \ll 1$ ), then, as follows from system (13), the order parameter phase differences on both Josephson contacts differ only slightly:

$$\varphi_a^* \approx \frac{\pi}{2}, \quad \varphi_b^* \approx \frac{\pi}{2}, \quad (16)$$

the critical current of the interferometer is close to the sum of the Josephson contact critical currents, and the magnetic flux created by this current is small

$$i_c \approx 1, \quad f_s \approx \frac{\alpha\beta}{2} \ll 1. \quad (17)$$

If the difference in the critical currents of the Josephson contacts is significant [ $\pi\beta(1 - |\alpha|) \ll 1$ ], then for such an interferometer (we assume  $I_b > I_a$  for definiteness)

$$\varphi_a^* \approx \frac{\pi}{2}(1 + 2\beta), \quad \varphi_b^* \approx \frac{\pi}{2}, \quad (18)$$

and, therefore, the critical current and the magnetic flux created by this current lie within

$$\alpha \leq i_c \leq 1, \quad \frac{\alpha\beta}{2} \leq f_s \leq \frac{\beta}{2}. \quad (19)$$

The considered interferometer is distinguished by a significant asymmetry of the Josephson contact critical currents. For such an interferometer, a change in the order parameter phase difference at a weak Josephson contact (at a "strong" Josephson contact, the phase difference is close to  $\pi/2$ ), as the current through the interferometer increases to the critical value, is shown in Fig. 2 for the characteristic values of the parameter  $\beta$ . The standard dependences of the interferometer critical current on the degree of asymmetry  $\alpha$  and parameter  $\beta$ , as well as the dependence of the magnetic flux  $f_s$  created by this current on parameter  $\beta$ , are shown in Figs. 3 and 4.

Figure 4 in particular shows how a significant increase in the magnetic flux  $f_s$  created by the difference in transport currents of the interferometer branches at  $\alpha = 0.55 - 0.75$  causes a significant decrease in its critical current  $i_c$  that corresponds to the considered model of interferometer processes. This means

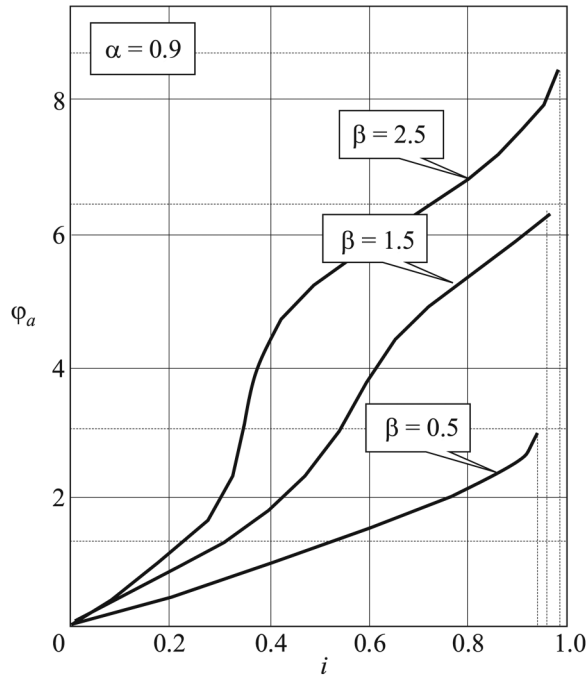


FIG. 2. The order parameter phase differences  $\varphi$  at the “weak” contact of the interferometer as a function of the current flowing through the interferometer.

that an increased flux excites an increased value of the circulating current in the interferometer, which leads to a decrease in the transport current required to achieve the critical state of the interferometer contacts.

Using the Eq. (9) for the magnetic flux and the wave function uniqueness condition (10), we obtain the connection between the magnetic flux and the order parameter phase difference at the

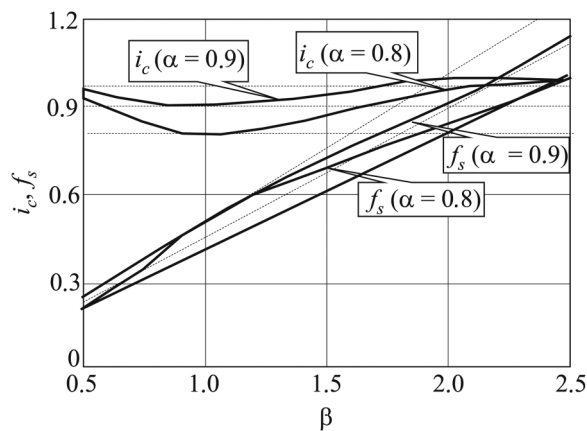


FIG. 3. The dependences of the critical current and the interferometer magnetic flux created by it, as functions of parameter  $\beta$ .

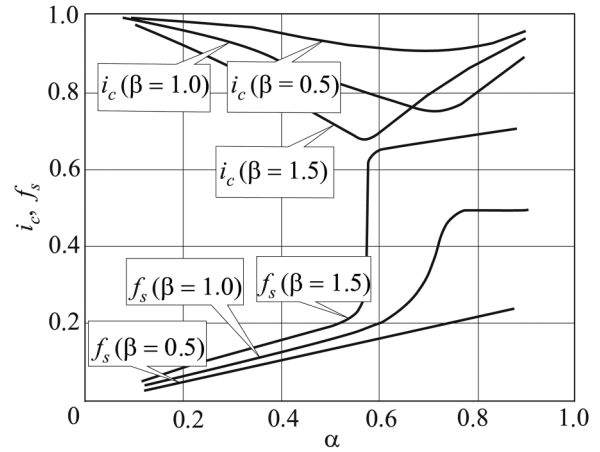


FIG. 4. The critical current and the interferometer magnetic flux it creates as functions of asymmetry.

Josephson contacts:

$$f_s = \beta \frac{(1 - \alpha) \sin(\varphi_b - 2\pi f_s) - (1 + \alpha) \sin \varphi_b}{4} = \beta \frac{(1 - \alpha) \sin \varphi_a - (1 + \alpha) \sin(\varphi_a - 2\pi f_s)}{4}. \quad (20)$$

Since for the interferometer under consideration, the asymmetry coefficient  $|\alpha|$  is close to one, it follows from Eq. (20) that the current through the interferometer is uniquely determined by the values of the order parameter phase differences at the Josephson contacts, if parameter  $\beta$  is such that the magnetic flux through the interferometer circuit created by the critical current is less than half of the flux quantum.<sup>8</sup>

Therefore, the values of the order parameter phase differences matching the critical current of the interferometer, correspond to the interferometer’s single quantum state with the critical current. As soon as the current through the interferometer exceeds the critical value, the Josephson contacts go into the resistive state, in which voltage appears, the current begins to flow into the shunt inductor, and the current through the interferometer begins to decrease. When the current through the interferometer drops to the critical value, the Josephson contacts again become superconducting and the flow of current into the shunt inductor stops. Thus, the current in the interferometer remains equal to the critical value, and the current in the shunt inductor increases in proportion to the growth of the transport current.

If the critical current in a highly asymmetric interferometer creates a magnetic flux through the interferometer circuit that is more than half the flux quantum, then different values of the magnetic flux through the interferometer circuit, and consequently different values of the current through the interferometer, can correspond to the same values of the order parameter phase differences. In particular, at least two interferometer quantum states

(for large values of  $\beta$  there may be several such states) match the values of the order parameter phase differences corresponding to the interferometer critical current. In one state the current is equal to the critical value, and in the other the current is  $\delta i$  less than critical. As the current through the interferometer increases above the critical value, a voltage appears at the Josephson contacts, the current begins to flow into the shunt inductor, and the current through the interferometer starts to drop. But now the reduction of the current through the interferometer, and therefore the current increase in the shunt inductor, occur until the interferometer switches to the quantum state with the lowest current. This quantum state of the interferometer exists until the current running through it reaches the critical value once more. To do this, obviously, the transport current must increase by  $\delta i$ . Thus, characteristic “steps” of the current form in the shunt inductor, the magnitude of which in the above values is equal to<sup>8</sup>

$$\delta i = \frac{1}{2\beta}. \tag{21}$$

In physical units, this corresponds to the condition for the appearance of discrete current switching in the interferometer and shunt inductor

$$\delta I_c = \delta I_1 \equiv \delta I = \frac{\Phi_0}{2L_0}. \tag{22}$$

At the same time, it seems to us that the switching process consists of two phenomena: the current, defined by the Eq. (22),

passes into the shunt inductor, but the flux in the interferometer changes by the flux quantum.

The moment the current jumps in the interferometer circuit, a voltage pulse of  $\delta u = \Phi_0/\tau$  is generated, where  $\tau$  is the relaxation time of the current state of the interferometer contacts. This pulse is directly related to the superconductor bandgap  $\delta u \approx \Delta/e$  and, therefore, the magnitude of the superconductor bandgap can be estimated by the formula

$$\Delta \approx e\delta u. \tag{23}$$

Since the interferometer’s standard transition time to a new quantum state is determined by the shunt circuit inductance  $L_1$ , it is much longer than the relaxation time

$$\delta t = \frac{L_1}{L_0} \tau, \tag{24}$$

and can easily be measured. Now, using the following estimate for interferometer inductance from Eq. (22) we get:

$$L_0 = \frac{1}{2\delta i} \frac{\Phi_0}{I_a + I_b}, \tag{25}$$

as well as a calculation formula for estimating the relaxation time

$$\tau = \frac{\Phi_0}{2L_1} \frac{\delta t}{\delta i(I_a + I_b)}. \tag{26}$$

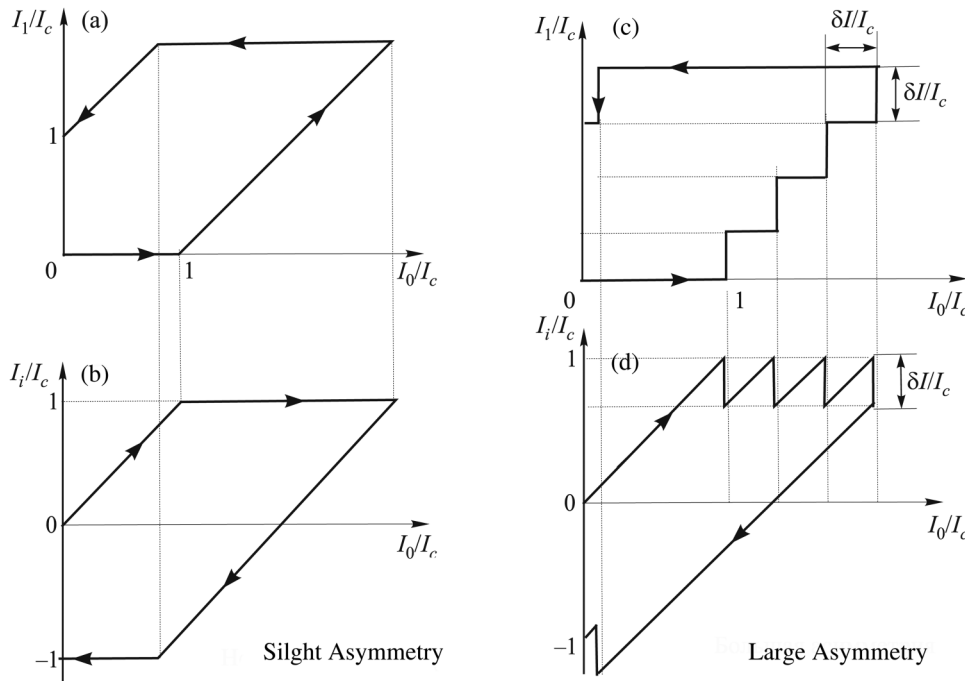
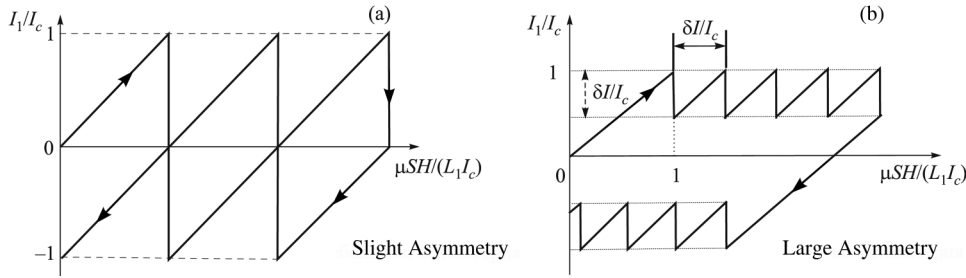


FIG. 5. The current in shunt inductance  $I_1/I_c$  and interferometer  $I/I_c$  as a function of the transport current.



**FIG. 6.** The current in the shunt inductor  $I_1/I_c$  as a function of the external magnetic field at a slight (a) and large (b) asymmetry. The current in the interferometer  $I/I_c$  coincides with the inductor current.

### 2.1. Controlling the transport current

Let us first consider a case when the current through the interferometer increases only due to a change in the transport current, and there is no external magnetic field.

As long as the transport current is less than the critical, the current in the interferometer increases, and the current in the shunt inductor is practically absent due to the Laue law.<sup>17</sup> Note that if the transport current is small, the currents in the arms of the interferometer are similar, and therefore, the magnetic flux through the interferometer circuit is negligible. As the transport current increases due to an increase in the parametric inductance<sup>18</sup> of the Josephson junctions, the difference in currents in the interferometer arms increases, and the magnetic flux through the interferometer circuit increases accordingly.

If the asymmetry of the interferometer is relatively small, and if the magnetic flux through the interferometer circuit does not exceed half of the flux quantum when the transport current is increased to a critical value, then there are no discrete changes in the current in the shunt inductor [Fig. 5(a)]. After reaching the critical value, the current in the interferometer remains equal to it, and the current in the shunt inductor increases in proportion to the growth of the transport current

$$I_1 = \begin{cases} 0, & I < I_c \\ I - I_c, & I > I_c \end{cases}, \quad I_i = \begin{cases} I, & I \leq I_c \\ I_c, & I > I_c \end{cases} \quad (27)$$

where  $I_c$  is the critical current of the interferometer.

If the transport current is then reduced, because the inductance of the interferometer is much less than the shunting inductance, the interferometer current begins to decrease, whereas the current in the shunt inductor does not change. After reducing the current in the interferometer to a negative critical value, the current in the shunt inductor starts to decrease, and when the transport current decreases to zero, a current that is equal to the critical current of the interferometer will remain in the shunt circuit. In this case, there is an opposite sign critical current in the interferometer [see Fig. 5(b)].

If the asymmetry of the interferometer is large enough, and the critical current creates a magnetic flux that is greater than half of the flux quantum, then when the interferometer's critical current is reached discrete jumps in the current manifest in the shunt inductor  $\delta I_1 = \delta I$  (22), accompanied by voltage pulses [Fig. 5(c)].

Such current surges in the shunt inductor begin when the transport current exceeds the critical value, have the value  $\delta I = \Phi_0 / (2L_0 I_c)$ , and occur every time the transport current

increases by  $\delta I$  ( $k = 1, 2, \dots$ ):

$$I_1 = \begin{cases} 0, & I \leq I_c \\ k\delta I, & k\delta I < I - I_c < (k + 1)\delta I, \end{cases} \quad (28)$$

$$I_i = \begin{cases} I, & I \leq I_c \\ I - (k + 1)\delta I, & k\delta I < I - I_c < (k + 1)\delta I. \end{cases}$$

If the transport current is decreased after it reaches a certain value, then because the inductance of the interferometer is much less than the shunt inductance, at first the magnetic flux in the interferometer circuit will decrease once it reaches the interferometer critical current, as will the screening current, respectively. A part of the transport current will pass from the shunt inductor to the interferometer, and the Josephson contacts will again be in the superconducting state. When the transport current decreases to zero, the current that was in the shunt circuit when the transport current was equal to  $I_0 = 2I_c$ , i.e. the current  $I_0$  equal to the interferometer critical current  $I_c$  [Fig. 5(d)], will remain there. It is this current that is recorded in the experiment.

Note that if the flux of the external magnetic field through the shunting inductance is non-zero, the nature of the current change

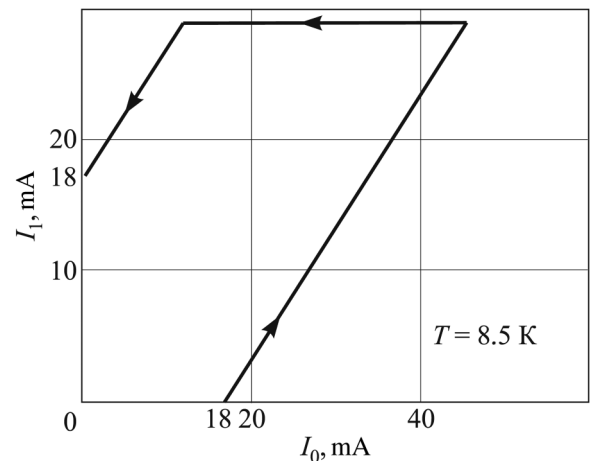


**FIG. 7** The current in the shunt circuit as a function of transport current, at a temperature of 8.5 K.

will remain the same, but current surges will begin at a lower or higher transport current, depending on the direction of the current in the shunt inductor, caused by the external field.

### 2.2. Controlling the external magnetic field

Let us now consider a case when the current through the interferometer  $I_i$  increases due to a change in the external magnetic field through the shunt inductor circuit.

If the asymmetry of the interferometer is slight, so that as the external magnetic field increases to the value at which the interferometer current reaches a critical value, the magnetic flux through its circuit does not exceed half of the magnetic flux quantum, and therefore, since the Josephson contacts went into the resistive state, the current in the shunt inductor drops to zero, and the Josephson contacts return to the superconducting state [Fig. 6(a)]. The current flowing through the interferometer obviously coincides with the current in the shunt inductor

$$I_1 = \frac{\mu S}{L_1} H - k I_c, \quad \frac{L_1 I_c}{\mu S} k < H < \frac{L_1 I_c}{\mu S} (k + 1), \quad k = 0, 1, 2 \dots, \quad (29)$$

where  $\mu = 4\pi \times 10^{-7}$  is the magnetic permeability of vacuum,  $S$  is the area of the shunt circuit,  $H$  is the external (orthogonal to the plane of the shunt circuit) magnetic field, and  $I_c$  is the critical current of the interferometer.

If the asymmetry of the interferometer is large enough for the external magnetic field to increase to the value at which the

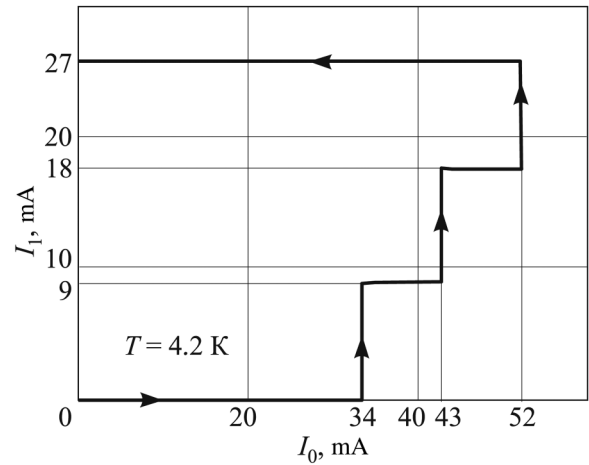


FIG. 8. The current in the shunt circuit as a function of transport current, at a temperature of 4.2 K.

interferometer current reaches a critical value, the magnetic flux through its circuit exceeds half the magnetic flux quantum, and then discrete current surges [Fig. 6(b)] occur in the shunt inductor when the interferometer critical value is reached. These current surges begin when the current through the interferometer exceeds the critical value, have the value  $\delta I$ , and occur every time the circulating current in the shunt inductor increases by  $\delta I$

$$I_1 = \begin{cases} \frac{\mu S}{L_1} H, & H < \frac{L_1 I_c}{\mu S}, \\ I_c - \delta I + \left( \frac{\mu S}{L_1 \delta I} H - k I_c \right), & \frac{L_1 I_c}{\mu S} \delta I k < H < \frac{L_1 I_c}{\mu S} \delta I (k + 1), \end{cases} \quad k = 1, 2, \dots \quad (30)$$

Note that if the transport current is nonzero with a change in the magnetic field, the nature of the current dependence in the shunt inductor remains the same, but obviously the current jumps begin at a different value of the magnetic field.

### 3. MODEL VERIFICATION

The circuit of the experimental interferometer was formed from a niobium micro wire with a diameter of 70  $\mu\text{m}$ , the ends of which were stacked crosswise and mechanically compressed. At the point where the wires crossed there was a Josephson clamped point contact. J. Zimmerman and A. Silver<sup>10</sup> were the first to notice that the microstructure of the clamped point contact is such that it usually represents a kind of ultraminiature superconducting quantum interferometer with several micro contacts of different critical currents, connected in parallel.

The highly inductive shunt circuit was made of a niobium microwire and contained two series-connected superconducting

coils. The sum of their inductances basically determined the geometric inductance of the shunt circuit, which was  $L_1 \approx 1.6 \times 10^{-6}$  H. One coil with an inductance of  $0.6 \times 10^{-6}$  H was wound on the core of a ferroprobe, which was designed to detect the current in the

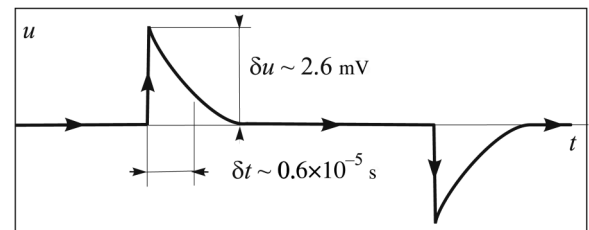


FIG. 9. Power surges on the shunt inductance based on transport current at a temperature of 4.2 K.

TABLE I. The data of experimentally obtained dependences.

Interferometer Temperature, K	Critical Current, mA	Current Surges in Shunt Inductor, mA	Power Surges in Shunt Inductor, mV	Pulse Duration in Shunt Inductor, $\mu$ s
8.5	$18 \pm 0.3$	—	—	—
4.2	$34 \pm 0.3$	$9 \pm 0.2$	$2.6 \pm 0.2$	$6 \pm 1$

shunt circuit by the magnitude of the magnetic field measured by ferroprobe. The second coil with an inductance of  $1.0 \times 10^{-6}$  H was the primary winding of a cryogenic pulse transformer, which was designed to convert a jump in the current in the shunt circuit into a voltage pulse on the secondary winding of the transformer.

The interferometer preparation and measurement methods are described in detail in Refs. 6–8, and Figs. 7–9 and in Table I show the experimentally obtained dependences of the current in the shunt circuit on the transport current, and the corresponding voltage jumps.

The dependence shown in Fig. 7 corresponds to the case of a “slight” asymmetry of the interferometer. This dependence was obtained by placing the interferometer in helium vapor, which caused its temperature to rise to 8.5 K and, consequently, led to a decrease in the Josephson contacts’ critical current and the magnetic flux generated by this critical current.

The growth of the current in the shunt circuit began when the transport current increased to  $I_c^{8.5} \approx 18$  mA; therefore, this is the critical current of the interferometer at  $T = 8.5$  K. Discrete current surges in the shunt circuit were not observed at this temperature, therefore, the magnetic flux created by this critical current was less than half of magnetic flux quantum, i.e. the inequality  $\Phi_x^{8.5} < \Phi_0/2$  is fulfilled.

The dependence shown in Fig. 8 corresponds a “large” asymmetry of the interferometer. This dependence was obtained at an interferometer temperature of 4.2 K. At this temperature, the Josephson contacts’ critical current increased and, accordingly, so did the generated magnetic flux. Current surges in the shunt circuit were  $\delta I_{4.2} \approx 9$  mA and started at a current of  $I_c^{4.2} \approx 34$  mA, which is obviously the critical current of the interferometer at  $T = 4.2$  K. At this current, there are discrete current surges in the shunt circuit, so the inequality  $\Phi_x^{4.2} < \Phi_0/2$  must be fulfilled. On the other hand, since the magnetic flux of the interferometer increases in proportion to the growth of the critical current, then  $\Phi_x^{4.2} \approx \frac{\Phi_0^{8.5} I_c^{4.2}}{I_c^{8.5}} < 0.95\Phi_0$  i.e. the magnetic flux created by the critical current at a temperature  $T = 4.2$  K did not exceed the flux quantum, which means that when the critical value of the current

in the interferometer circuit was reached, the flux changed only by one flux quantum.

The normal resistance of an isolated Josephson clamped point contact measured by the traditional four-probe method was about  $R_n \approx 0.25 \Omega$ , which makes it possible to estimate the diameter of its “spot” as  $d \approx 4 \times 10^{-8}$  m. Since the distance between Josephson contacts in the interferometer under consideration is comparable with their diameters, its inductance is  $L_0 > 0.4 \times 10^{-13}$  H.<sup>8</sup>

To estimate the inductance of the interferometer according to the experimental results, it is possible to use the formula  $L_0 = \Phi_0/2\delta I \approx 1.1 \times 10^{-13}$  H, and the obtained result complies with the above inductance estimate.

Figure 9 shows an oscillogram of voltage surges on the shunt circuit. The magnitude of the voltage jumps was  $\delta u \approx 2.6$  mV, making the niobium bandgap  $\Delta \approx e\delta u \approx 2.6$  meV, which is close to the value  $\Delta \approx 2.8$  meV that was measured by the tunneling method.<sup>19</sup>

Finally, the relaxation time at the measured duration  $\delta t = 0.6 \times 10^{-5}$  s of the voltage pulse on the shunt inductor  $\tau \approx (\Phi_0/2L_1)(\delta t/\delta I) \approx 0.4 \times 10^{-12}$ , which is close to the estimated estimate of this value, given in Ref. 12.

The results of the calculations and their comparison with the literature data are given in Table II.

Figure 10 shows a current in the shunt circuit as a function of the external magnetic field, obtained in another experiment<sup>7</sup> (the figure shows the current in the coil that is creating the field). This dependence was obtained at  $T = 4.2$  K and corresponds to the case of a “large” interferometer asymmetry. To create a magnetic field above the surface of the shunt circuit, the coil with the current that was creating the field was specifically placed, and to weaken the influence of random external magnetic fields, the location of the structure in question was screened with a ferromagnetic shield.

The current surges in the shunt inductor were  $\delta I \approx 6.0$  mA at an interferometer critical current  $I_c^{4.2} \approx 18$  mA.

The interferometer inductance calculated according to the results of the experiment is  $L_0 \approx 1.7 \times 10^{-13}$  H, which complies with the inductance estimate obtained from geometrical considerations.

TABLE II. Calculation results versus literature data.

Calculated Interferometer Inductance, pH	Calculated Relaxation Time, $\mu$ s	Calculated Bandgap, meV
0.06–0.18 ( $> 0.04$ , according to data from Ref. 8)	$0.4 \times 10^{-12}$ ( $10^{-12}$ , according to data from Ref. 12)	2.6 (2.8, according to data from Ref. 19)



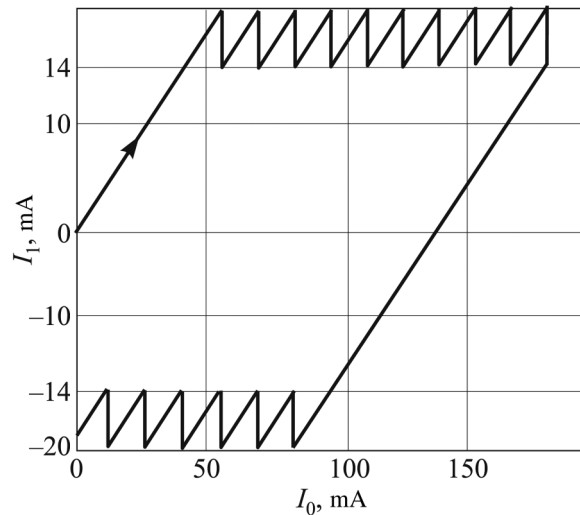


**FIG. 10.** The dependence of the current in the shunt inductor on the current exciting the magnetic field.

#### 4. CONCLUSIONS

A mathematical model of the current flow in an asymmetric dc superconducting quantum interferometer based on a clamped contact shunted by an inductive superconducting circuit is constructed.

The criterion for the manifestation of discrete quantum current transitions from the interferometer to the shunt inductor is determined.

The dependences of the current in the shunt inductor on the transport current and the external magnetic field are explained.

The verification of the model by comparing the calculated dependences against those that were experimentally determined, shows the agreement between the two.

#### REFERENCES

- <sup>1</sup>S. I. Bondarenko, B. I. Verkin, E. A. Golovanev, V. V. Kravchenko, and P. P. Pavlov, *Collection Geophysical Equipment* **69**, 3 (1979).
- <sup>2</sup>B. I. Verkin, S. I. Bondarenko, V. V. Stogny, V. N. Fenchenko, and V. I. Sheremet, Y. Y. Biezays, *Geology and Geophysics* **11**, 42 (1980).
- <sup>3</sup>B. I. Verkin, S. I. Bondarenko, Y. F. Karev, N. N. Romanov, V. N. Fenchenko, *Geology and Geophysics* **11**, 36 (1981).
- <sup>4</sup>B. I. Verkin, S. I. Bondarenko, A. V. Lukashenko, A. A. Shablo, I. V. Svechkarev, G. E. Kurilov, and V. A. Komashko, *Fiz. Nizk. Temp.* **13**, 998 (1987) [*Low Temp. Phys.* **13**, 576 (1987)].
- <sup>5</sup>H. Suzuki, *News Lett. Supercond. Electron.* **3**, 3 (2009).
- <sup>6</sup>V. P. Koverya, S. I. Bondarenko, A. V. Krevsun, NM Levchenko, and I. S. Bondareko, *Fiz. Nizk. Temp.* **36**, 759 (2010) [*Low Temp. Phys.* **36**, 605 (2010)].
- <sup>7</sup>V. P. Koverya, A. V. Krevsun, S. I. Bondarenko, and NM Levchenko, *Fiz. Nizk. Temp.* **38**, 44 (2012) [*Low Temp. Phys.* **38**, 35 (2012)].
- <sup>8</sup>S. I. Bondarenko, V. P. Koverya, A. V. Krevsun, and L. V. Gnezdilova, *Fiz. Nizk. Temp.* **41**, 235 (2015) [*Low Temp. Phys.* **41**, 179 (2015)].
- <sup>9</sup>B. D. Josephson, *Phys. Lett.* **1**, 251 (1962).
- <sup>10</sup>A. H. Silver and J. E. Zimmerman, *Phys. Rev. Lett.* **15**, 888 (1965).
- <sup>11</sup>J. E. Zimmerman and A. H. Silver, *Phys. Rev.* **141**, 367 (1966).
- <sup>12</sup>A. H. Silver and J. E. Zimmerman, *Phys. Rev.* **157**, 317 (1967).
- <sup>13</sup>H. Frohlich, H. Koch, W. Vodel, D. Wachter, und O. Frauenberger, *Wissenschaftliche Zeitschrift* **1/2**, 197 (1973).
- <sup>14</sup>A. T. A. M. De Waele and R. De Bruyn Ouboter, *Physica* **41**, 225 (1969).
- <sup>15</sup>T. A. Fulton, L. N. Dunkleberger, and R. C. Dynes, *Phys. Rev. B* **6**, 855 (1972).
- <sup>16</sup>M. T. Heath, *Scientific Computing: An Introductory Survey* (McGraw-Hill, 2005).
- <sup>17</sup>D. B. Sullivan and J. E. Zimmerman, *Am. J. Phys.* **39**, 1504 (1971).
- <sup>18</sup>K. K. Likharev and B. T. Ulrich, *Systems with Josephson Contacts* (Publishing House of Moscow University, Moscow, 1978).
- <sup>19</sup>P. Townsend and J. Sutton, *Phys. Rev.* **128**, 591 (1962).

Translated by [AIP Author Services](#)